Supporting Information

Xu et al. 10.1073/pnas.1419533112

SI Materials and Methods

Mice were housed in a temperature and climate-controlled facility on a 12-h light/dark schedule. Adult male mice (3–4 mo), backcrossed to >N4 onto C57BL/6, were used in all experiments.

Immunotoxin Ablation. A targeted immunotoxin, ChAT-saporin (ChAT-SAP) (Advanced Targeting Systems, IT-42) and with a negative control, saporin conjugated to nonspecific IgG (IgG-SAP) (Advanced Targeting Systems, IT-35), were infused into the dorsal striatum of male wild-type C57BL/6 mice (The Jackson Laboratories), using standard stereotaxic technique. Target coordinates were anterior-posterior (AP) 0.7 mm, medial-lateral (ML) ± 2.3 mm, dorsal-ventral (DV) −3.5 mm. A total of 0.3 μL of ChAT-SAP was injected into mouse striatum with a dose of 0.3 μg/μL at a flow rate of 0.1 μL/min using 2 μL Hamilton syringe attached to a micropump [UltramicroPump II; World Precision Instruments (WPI)], whereas control mice were equivalently injected with IgG-SAP. Mice were euthanized and their brains rapidly removed 1 wk after the toxin injection. Brains were sliced, equilibrated in a sucrose solution, and sliced on a cryostat. Brain slices were immunostained using goat anti-ChAT primary antibody (Millipore: AB144P) 1:500 and biotinylated rabbit anti-goat Ig secondary antibody (Vector Laboratories; BA-5000) at 1:1,000, followed by diaminobenzidine immunoperoxidase development using the Vectastain Elite ABC kit (Vector Laboratories) and the DAB substrate kit for peroxidase (Vector Laboratories), according to the manufacturer's instructions; immunostaining was performed using rabbit serum.

Unfortunately, whereas ChAT interneuron ablation was apparent after ChAT-SAP, we also found reductions in ChAT immunoreactivity, qualitative changes in ChAT cell morphology, and patchy cell loss after treatment with IgG-SAP, even at low doses (Fig. S1). Both ChAT-SAP and IgG-SAP also led to prominent microgliosis throughout the striatum. This calls into question the specificity of such reagents, at least in mice. This motivated us to design a targeting system for more specific and controlled interneuronal ablation.

Vector Constructs and Adeno-Associated Virus Production. Diphtheria toxin (DT) induces apoptosis with extraordinary efficiency (1), but it cannot normally enter rodent cells. Expression of the simian diphtheria toxin receptor (sDTR) renders mouse cells sensitive to ablation after systemic DT (2). We developed a combinatorial approach to restrict sDTR, fused to a flu antigen (FLAG) epitope for ready immunohistochemical identification, to ChAT interneurons of the dorsal striatum (Fig. 1*A*).

We used a modified FLEX cassette (Fig. 1*A*) to invert eGFP and DTR-FLAG in the presence of *Cre*-recombinase. The promoter/enhancer combination used to drive expression included the elongation factor 1a promoter and the 3′ enhancer woodchuck hepatitis virus posttranscriptional regulatory element. We used a modified FLEX cassette with two pairs of inverted *cre*-recognition sites (*loxP* and *lox2722*) (3) to invert eGFP and DTR-FLAG, and delete eGFP, in the presence of *cre*-recombinase, such that DTR-FLAG is brought into the sense orientation and is expressed from the EF-1 promoter. *Cre*-expressing cells are thus made susceptible to ablation by systemic administration of DT (2).

eGFP was inserted in between the loxP and lox 2722 sites at the 5′ end of the FLEX cassette. The simian diphtheria toxin receptor (DTR) gene, labeled at its C-terminal with a flu antigen (FLAG) epitope tag, was placed within the FLEX cassette in the antisense orientation. In the presence of *Cre*-recombinase this cassette inverts, such that DTR-FLAG is brought into register with the EF-1a promoter, and the eGFP gene is deleted. (We found eGFP deletion to be necessary for optimal DTR expression, presumably because the antisense eGFP gene in the 3′ untranslated region of the DTR mRNA after *Cre*-mediated flipping interferes with efficient translation.)

This construct expression cassette was packaged into adeno-associated virus (AAV) rh10 serotype by the Salk Institute Viral Vector Core (vectorcore.salk.edu) with a titer of 1×10^{13} genomic copies per milliliter, as measured by real-time PCR.

We also designed a control vector, C06, as shown in Fig. 1*A*, which has very similar sequence as A06 but with muptiple point mutations in the 3′ loxP and lox 2722 sites, preventing Cre-mediated inversion. The sequence below shows with bold letters indicating mutations: ATAACTTCGTATA**AAAAAAAAA**TATAC-GAAGTTATTTGCCTTAACCCAGAAATTATCACTGTTAT-TCTTTAGAATGGTGCAAAGAATAACTTCGTATA**CCCCCC-CCC**TATACGAAGTTAT. C06-infected cells thus always express eGFP and never express DTR, irrespective of Cre-expression.

In Vitro Transfection. These constructs were tested in vitro using transient transfection. Neuro-2a mouse neuroblastoma cells (ATCC) were cultured in a 12-well plate in complete growth culture media DMEM (Gibco). Transient transfections were performed using Lipofectamine LTX (Life Technologies), following the manufacturer's instructions. For each transfected well, 1 μg DNA and 1 μL PLUS were added to 200 μL Opti-MEM medium, mixed, and incubated at room temperature for 5 min. A total of 4 μL of Lipofectamine LTX was added, and the mixture was allowed to sit for 25 min. The mixture was then added to each well. At 48 h later, cells were rinsed with PBS and fixed with 1% paraformaldehyde/PBS solution at 4 °C overnight before immunostaining, as detailed below.

A total of 0.5 μg of each plasmid was used for each transfection. For conditions in which only one plasmid was transfected, an additional 0.5 μg plasmid DNA (pUC) was added, such that a total of 1 μg DNA was used for each transfection. Note that transfected *Cre*-recombinase was fused to eGFP; green fluorescence in these experiments (Fig. 1*B*) therefore reflects both eGFP expression from the A06 or C06 construct and *Cre*-expression.

In Vivo Viral Infusion and Virus Validation. Adult male hemizygous ChAT-*cre* transgenic mice were produced in our vivarium by crossing heterozygous male Chattm1(*cre*)Lowl mice (www.jax.org: 006410) with female wild-type C57BL/6 mice (The Jackson Laboratories). Stereotaxic surgery was performed following standard procedures, under sterile conditions. ChAT-*cre* mice were anesthetized with an i.p. injection of xylazine (10 mg/kg; Bayer Pharma) and ketamine (100 mg/kg; Merial) and placed into a mouse stereotaxic apparatus. A 2-μL Hamilton syringe attached to a micropump (UltramicroPump II; WPI) was lowered through a skull burr hole into the striatum at the coordinates: DLS (AP + 0.8 mm; ML ± 2.3 mm; DV −3.5 mm relative to bregma) or DMS (AP + 0.9 mm; ML ± 1.5 mm; DV −3.5 mm), with reference to the atlas of Paxinos (4). A total of 0.4 μL (for DLS) or 0.27 μL (for DMS) of virus was infused bilaterally at a flow rate of 0.1 μL/min. The Hamilton syringe was left in place for 10 min after completion of the infusion to eliminate back-flow and then slowly withdrawn. This process was repeated on the other side to produce bilateral viral injections. Mice were then sutured and returned to their home cage for a minimum of 2 wk postsurgery.

For validation experiments (Fig. 2), mice received A06 virus on one side and C06 contralaterally. Some mice in validation experiments were killed 2 wk later, without administration of DT (Calbiochem, 15 μg/kg i.p.; Fig. 2 *A* and *D*). In all other experiments (Figs. 2 *B* and *C*, 3, and 4), mice received a single DT i.p. injection at a dose of 15 μg/kg. This dose was empirically determined to produce efficient interneuronal ablation (Figs. 2*C* and 3 *B* and *E*) without any detectable histological or behavioral effects in C06-infused transgenic mice or in wild-type animals. Higher doses (40 μg/kg) impaired animals' startle response in a PPI assay, raising concerns that there might be other nonspecific effects.

A separate cohort of four mice was identically treated for qPCR validation of ChAT interneuron ablation (Fig. 2*E*), as further described below.

Immunohistochemistry. Mouse brains were rapidly dissected and fixed overnight in 4% (mass/vol) paraformaldehyde/PBS solution at 4 °C. After fixation, brains were equilibrated with 30% (mass/vol) sucrose/PBS. Frozen coronal sections were cut at 40 μm in six continuous slide sets throughout the striatum, such that each set sampled the brain at ∼250-μm intervals, and stored in cryoprotectant solution [30% (vol/vol) glycerin, 30% (vol/vol) ethylene glycol, 0.2× PBS solution] at 4 °C. Sections were immunostained following standard protocols. Briefly, brain sections were blocked in PBS with 10% (vol/vol) rabbit or donkey or goat serum, 0.2% Triton X, and 0.1% Tween 20 for 30 min at room temperature. Floating brain sections were stained with primary antibody in 1× PBS, 0.2% Triton X, and 0.1% Tween 20 + 5× rabbit or donkey or goat serum overnight at 4 °C, rinsed three times for 10 min with PBS at room temperature, stained with secondary antibody in 1× PBS, 0.2% Triton X, and 0.1% Tween 20 + 10× serum for 1 h at room temperature, and again rinsed three times for 10 min with PBS. Primary antibodies included goat anti-ChAT primary antibody (1:500; Millipore, AB144P), mouse anti-FLAG (1:500; Sigma, F1804), and chicken anti-GFP (1:2,000; Abcam, Ab13970).

For cell counting, ChAT was visualized (Fig. 3 *B* and *F* and Fig. S3) using goat anti-ChAT primary antibody (Millipore, AB144P) 1:500 and biotinylated rabbit anti-goat Ig second antibody (Vector Laboratories, BA-5000) at 1:1,000 followed by diaminobenzidine immunoperoxidase development using the Vectastain Elite ABC kit (Vector Laboratories) and the DAB substrate kit for peroxidase (Vector Laboratories), according to the manufacturer's instructions; immunostaining was performed using rabbit serum. Within each section the boundaries of the striatum were established using anatomical markers (chiefly the internal capsule and other white matter tracks; ref. 4), and ChAT-positive neurons within striatum were counted bilaterally in each section where this structure was present throughout the series. About five sections per mouse were then examined. Because of the relatively small number of total ChAT interneurons in the striatum, we counted all visible ChAT-positive cells rather than performing a stereological analysis. DMS and DLS were defined by arbitrarily dividing the striatum in two at its midpoint with a dorsal–ventral line. Data reported describe the number of ChAT-positive neurons counted in the DLS (Fig. 3*B*) or DMS (Fig. 3*E*), and demonstrate the extent of depletion of ChAT-positive cells in lesioned mice relative to controls. Cell counting was performed using Stereoinvestigator (MBF Biosciences).

For fluorescent staining (Figs. 1 and 2), primary antibodies were mouse anti-FLAG (1:500; Sigma F1804), chicken anti-GFP (1:2,000; Abcam, Ab13970) and goat anti-ChAT (1:500; Millipore, AB144P). Second antibodies were Alexa Fluor 594-conjugated donkey anti-mouse (1:400; Life Technologies, A21203), Dylight 488-conjugated donkey anti-chicken (1:400; Jackson Immunoresearch, 97336), and Alexa Fluor 633-conjugated donkey anti-goat (1:400; Life Technologies, A21082) were used; staining was performed using donkey serum. For apoptosis staining, rabbit anti-caspase 3 primary antibody (1:1,000; Abcam, AB44974) and Alexa Fluor 594-conjugated goat anti-rabbit (1:400; Life Technologies, A11037) were used, in goat serum. Confocal images (Fig. 2 *A*–*C*) were taken using a laser scanning confocal microscope (Olympus Fluoview FV300) at 200×. Fluorescent images (Fig. 1*B*) were taken with a Zeiss fluorescent microscope.

qPCR Expression Analysis. Mice ($n = 4$) were killed 15 d following DT injection. Striatum was rapidly dissected on ice. Tissue was stored at −80 °C for subsequent RNA isolation. RNA was isolated using the RNeasy Plus Mini kit (Qiagen), according to the manufacturer's instructions. RNA was reverse transcribed using SuperScript III (Life Technologies), and expression levels were evaluated with OneStep qPCR (Applied Biosystems) using SYBR Power Green (Applied Biosystems). GAPDH was used as the reference gene and analysis was performed using the ddCt method. Primer sequences are presented in Table S1.

Behavioral Analysis. For behavioral analysis, viruses were bilaterally infused into DLS or DMS, using the coordinates above; A06 was infused bilaterally for ablation animals and C06 for control animals. Age-matched male ChAT-cre transgenic mice were randomly assigned to receive either C06 or A06 virus. DT (15 μg/kg) was injected 14–15 d after surgery; behavioral analysis began 1 wk later. All brains were examined histologically after the completion of behavioral experiments, as described below; extent of viral spread (Fig. 3 *A* and *D* and Fig. S2) and ChAT interneuron ablation (Fig. 3 *B* and *E* and Fig. S3) were assayed; animals in which the virus was mistargeted were to be excluded, but no animals had to be excluded from either cohort. In DLS behavioral experiments (Figs. 3 and 4), $n = 5$ C06-infused control animals, $n = 6$ A06-infused ablation animals (after one C06-infused animal died postsurgery). In DMS behavioral experiments (Figs. 3 and 4), $n = 6$ C06-infused control animals and $n = 7$ A06-ablation animals (after one C06-infused animal died postsurgery). This group size was chosen because groups of this size have been sufficient to reveal stereotypy in an independent animal model (5).

Elevated Plus Maze and Open Field. The elevated plus maze test and the open field test were performed as previously described (5). Animals' exploratory activity was recorded using an overhead video camera connected to a computer. The Anymaze video tracking system (Stoelting) was used to measure the time spent in the open arms in 5 min in the elevated plus maze test and the time spend in the center zone and total distance traveled during a 10-min monitoring session in the open field test. The apparatus was thoroughly cleaned with 70% ethanol before each mouse was tested. The data analysis was done with Anymaze software by an investigator blind to experimental condition.

The open field test was done as previously described (6). Mice were placed into a clean Plexiglass box, 50 cm × 50 cm, with no bedding, under moderate intensity indirect illumination. Locomotor exploratory activity over 10 min was quantified using an overhead camera and the Anymaze video tracking system. Time spent in the central zone (25 cm × 25 cm) was quantified as an additional index of anxiety.

Prepulse Inhibition of Acoustic Startle. PPI was tested in an acoustic startle chamber (San Diego Instruments) using SR Lab startle response software as described previously (5, 7). Each mouse was placed into a Plexiglass cylinder attached to a piezoelectric sensor. The startle response to an acoustic stimulus was measured in the presence of a 65-dB white noise background that began a 5-min acclimation period. Each session consisted of four continuous block designs of a total of 65 trials that presented a 20-ms prepulse of 6, 12, or 16 dB above background white noise followed 200-ms later by either a 40-ms 120-dB startle

pulse or no pulse at all (null). Blocks 1 and 4 consisted of six consecutive pulse-alone trials, whereas blocks 2 and 3 each consisted of six pulse-alone trials, five of each kind of prepulse trial, and five no-stimulus trials, intermingled in pseudorandom order. The intertrial interval (ITI) averaged 15 s but was pseudorandomized during presentations. Startle magnitude was calculated as the average response to all of the pulse-alone trials in each block. Percentage of PPI was calculated as a percentage score in startle response caused by presentation of the prepulse according to the following formula: % PPI = 100 − [(mean startle response for prepulse-pulse trial)/(mean startle response for pulse-alone trial)] × 100. Initial analysis was performed blind to experimental condition.

Rotarod. Motor learning was assessed with an Med Associates rotarod machine. The rotation rate was increased from 4 to 40 rpm over 5 min. Five animals were tested concurrently in separate 6-cm-wide compartments, on a rod that was ∼3 cm in diameter and was elevated 16.5 cm. Each animal was assessed over three trials per day with 20-min ITIs and trained for 2 d. Latency to fall from the rod was recorded. Latency to fall in the first trial was analyzed by *t* test, to assess basal motor function/coordination. Latency to fall across trials was analyzed by RM-ANOVA, to assess motor learning. The investigator performing this experiment was blind to experimental condition.

Startle-Induced Stress. We noted repetitive grooming in ChAT interneuron-ablated animals after PPI during pilot experiments. We therefore used repeated unpredictable presentation of the acoustic startle stimulus as a mild stressor. Mice were placed in a clear-sided Plexiglass box (28 cm × 17 cm × 21 cm) within the sound-attenuating chambers where PPI is performed; the door was left open (for better visual monitoring) and the plastic cylinder within which mice are constrained during PPI was removed. Mice were acclimated to the box for 10 min, then a pseudorandom series of startle stimuli, identical to our PPI protocol (5, 7), was run for 13 min. Mice were visually monitored before, during, and for 30 min after this stressor. The whole process was videotaped and manually scored by an observer blind to experimental condition assignments. Time spent in repetitive behaviors, which consisted primarily of increased grooming, was scaled to a 10-min block for each stage; between-group comparisons were performed by *t* test.

Amphetamine-Induced Locomotion and Stereotypical Behaviors. D-amphetamine (AMPH) (Sigma) was dissolved in sterile 0.9% saline and injected intraperitoneally at 7 mg/kg. This dose was found in pilot experiments to be at the threshold for the production of substantial stereotypies in mice of this genetic background and have been selected for its effectiveness in activating locomotor behavior and for its discriminating effects in mouse models reproducing stereotype behavior. Baseline locomotor data and stereotypical behaviors were collected 10 min before AMPH (7 mg/kg, i.p.) treatment and mice were monitored for at least 60 min following injection of AMPH to determine whether mice expressed stereotypy behavior. The whole process was videotaped and automatically scored with the Cleversys system using a side camera, then manually checked by an observer unaware of treatment assignments (Fig. S4*C*).

Statistical Analysis. Data were organized using Microsoft Excel and analyzed using SPSS (IBM). No datasets violated normality assumptions; two-tailed parametric statistics were used in all cases, and the threshold for significance was set at alpha = 0.05. Student's *t* test or repeated-measure ANOVA were used, as appropriate and as described in the text. For repeated-measures behavioral data (Fig. 3 *C*, *D*, *G*, and *H*), data are collapsed across 30-min blocks following amphetamine stimulation for presentation and for post hoc analysis; however, the primary analysis used all data in 5-min bins in a repeated-measures ANOVA (Figs. S4 and S5).

1. Yamaizumi M, Mekada E, Uchida T, Okada Y (1978) One molecule of diphtheria toxin fragment A introduced into a cell can kill the cell. *Cell* 15(1):245–250.
2. Buch T, et al. (2005) A Cre-inducible diphtheria toxin receptor mediates cell lineage ablation after toxin administration. *Nat Methods* 2(6):419–426.
3. Sohal VS, Zhang F, Yizhar O, Deisseroth K (2009) Parvalbumin neurons and gamma rhythms enhance cortical circuit performance. *Nature* 459(7247):698–702.
4. Paxinos G, Franklin KBJ (2012) *The Mouse Brain in Stereotaxic Coordinates* (Academic, San Diego), 4th Ed.
5. Castellan Baldan L, et al. (2014) Histidine decarboxylase deficiency causes tourette syndrome: Parallel findings in humans and mice. *Neuron* 81(1):77–90.
6. Lee AS, Duman RS, Pittenger C (2008) A double dissociation revealing bidirectional competition between striatum and hippocampus during learning. *Proc Natl Acad Sci USA* 105(44):17163–17168.
7. Baldan Ramsey LC, Xu M, Wood N, Pittenger C (2011) Lesions of the dorsomedial striatum disrupt prepulse inhibition. *Neuroscience* 180:222–228.

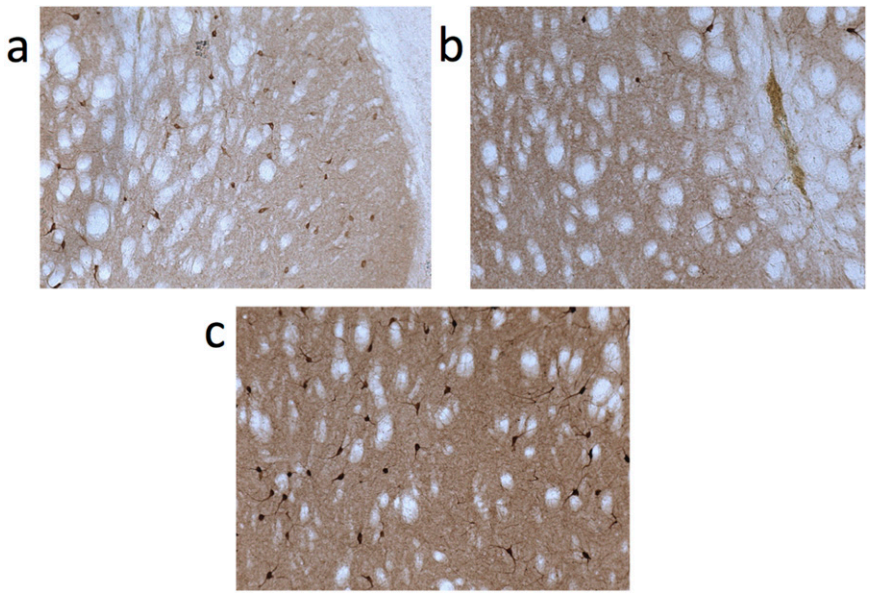

Fig. S1. Nonspecific ChAT interneuronal damage after infusion of negative-control IgG-conjugated saporin. A total of 0.3 μL IgG-SAP at 0.3 μg/μL was infused into mouse striatum. (*A*) ChAT immunoreactivity was reduced and interneuronal morphology was qualitatively altered by this negative control reagent (compare with *C*). (*B*) Patchy loss of ChAT interneurons after IgG-SAP infusion, revealed by ChAT immunostaining. (*C*) Normal ChAT staining and morphology in saline-infused control mice. This interneuronal damage in the negative control condition, which strongly suggests that damage to other cell types may also be occurring, problematizes the use of Ig-conjugated saporin as a strategy for interneuronal ablation in mice.

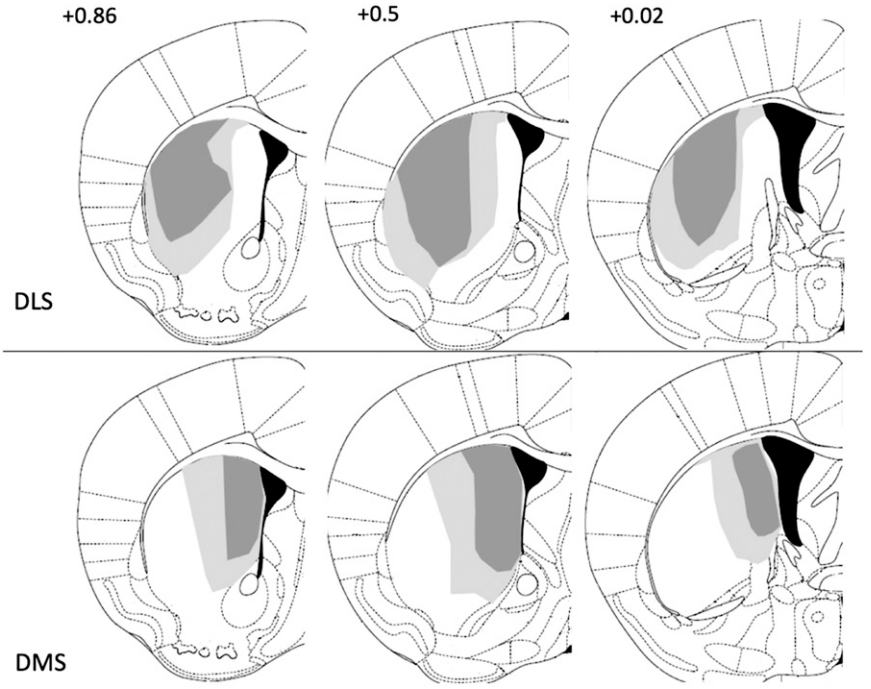

Fig. S2. Minimum and maximum extent of AAV-infected areas in mice used for behavioral analysis (Figs. 3, 4, and 5), as documented by eGFP expression.

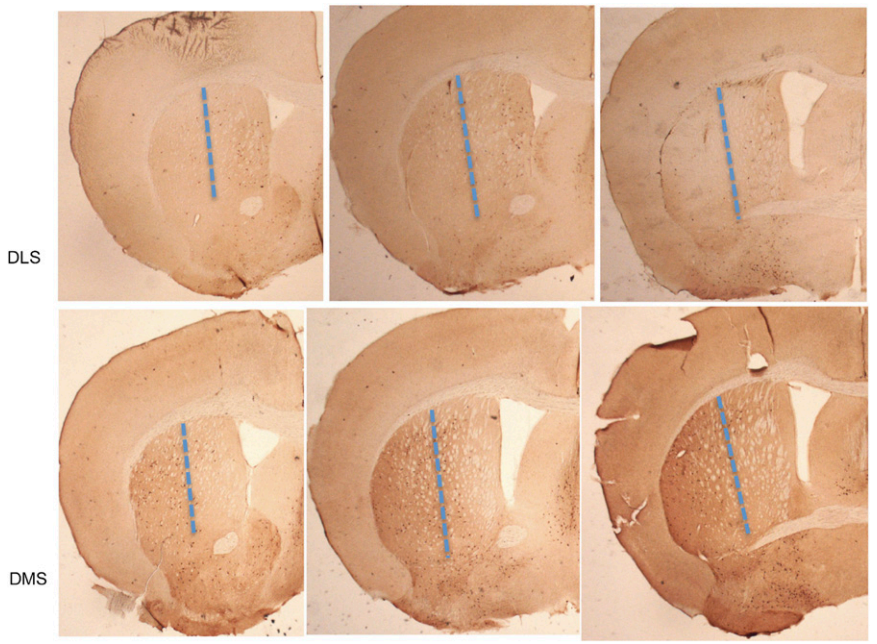

Fig. S3. Representative ChAT interneuron distribution in the striatum after DT-mediated ablation. ChAT immunoreactivity was visualized using diaminobenzidine. As there is no anatomical boundary between DLS and DMS, for purposes of quantification we arbitrarily divided the dorsal striatum down the middle, as shown, based on anatomical criteria. Cells were counted laterally to this line for quantification of DLS ChAT interneuron ablation (Fig. 3*B*) and medially to it for quantification of DMS ablation (Fig. 3*E*). Of note, ablation remained statistically significant when cells were counted across the entire striatum, although the absolute difference between the ablated and control condition was reduced because of the inclusion of nontargeted subregions.

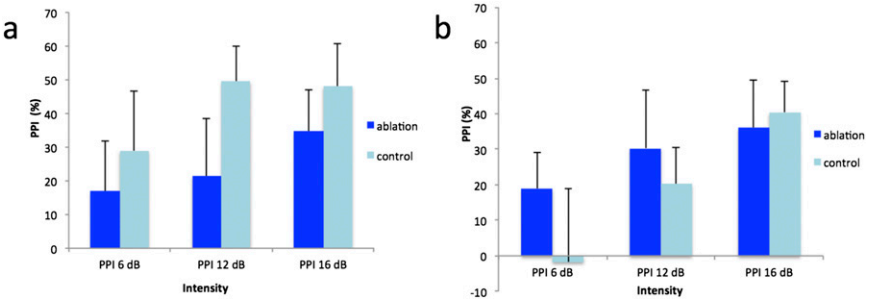

Fig. S4. Prepulse inhibition in DLS- and DMS ChAT-ablated mice. PPI was tested as previously described (5, 7) using three prepulse intensities. (*A*) There was no significant PPI deficit after DLS ChAT interneuronal ablation. $n = 6$ DLS ablated, 5 control; RM-ANOVA: main effect of intensity, $F(2,18) = 3.7$, $P = 0.047$; main effect of group, $F(1,9) = 0.87$, $P = 0.38$; intensity × group interaction $F(2,18) = 0.82$, $P = 0.46$. The nominally lower PPI in the ablated group resulted from two animals with very low PPI in this group; ablation in these two animals did not differ in either location or density from the rest of the group. (*B*) There was no deficit in PPI after DMS ChAT interneuronal ablation. $n = 7$ DMS ablated, 6 control; RM-ANOVA: main effect of intensity, $F(2,22) = 7.7$, $P = 0.003$; main effect of group, $F(1,11) = 0.25$, $P = 0.63$; intensity × group interaction, $F(2,22) = 1.4$, $P = 0.27$.

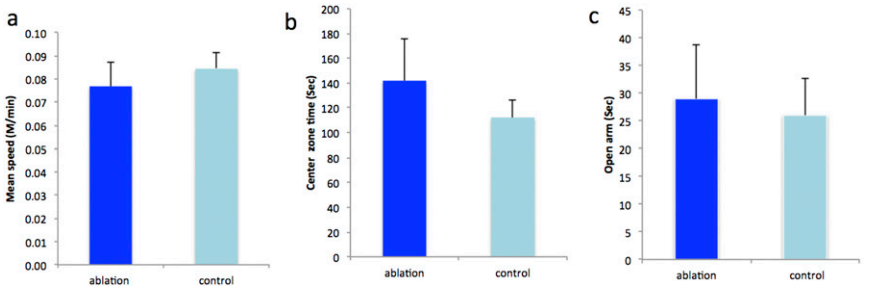

Fig. S5. Locomotion and anxiety in DLS ChAT-ablated mice. (*A*) Locomotor activity in a novel open field was unaltered by DLS ChAT interneuronal ablation (Student's *t* test, $P = 0.67$). (*B*) Center occupancy time, a measure of anxiety, was not altered by interneuronal ablation (Student's *t* test, $P = 0.21$). (*C*) Anxiety in the elevated plus maze, measured as time spent in the open arms over the course of a 5-min session, was not altered by interneuronal ablation (Student's *t* test $P = 0.13$).

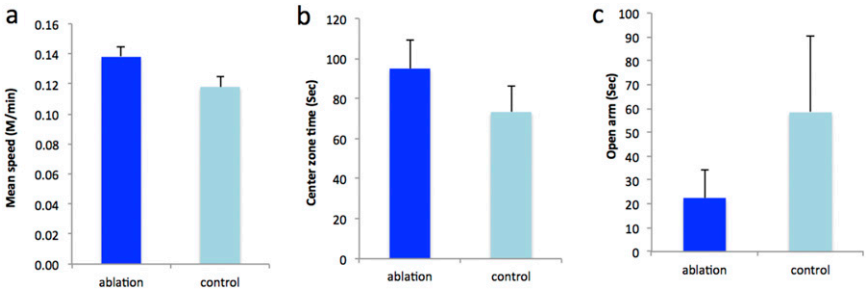

Fig. S6. Locomotion and anxiety in DMS ChAT-ablated mice. (*A*) Locomotor activity in a novel open field showed a slight nominal elevation after DMS ChAT interneuronal ablation, although this did not reach statistical significance (Student's *t* test, $P = 0.08$). (*B*) Center occupancy time, a measure of anxiety, was not altered by interneuronal ablation (Student's *t* test, $P = 0.29$). (*C*) Anxiety in the elevated plus maze, measured as time spent in the open arms over the course of a 5-min session, was not altered by interneuronal ablation (Student's *t* test $P = 0.28$).

Table S1. Primers used for qPCR analysis

Names	Forward	Reverse
GAPDH	AGGTCGGTGTGAACGGATTTG	TGTAGACCATGTAGTTGAGGTCA
CHAT	GGCCATTGTGAAGCGGTTTG	GCCAGGCGGTTGTTTAGATACA
SLC5A7	ATGTCTTTCCACGTAGAAGGACT	TTGCCGCTGTTTTTGGTTTTC
NTRK1	GCCTAACCATCGTGAAGAGTG	CCAACGCATTGGAGGACAGAT
GAD1	AACGTATGATACTTGGTGTGGC	CCAGGCTATTGGTCCTTTGTAAG
KCNC1	TCAACCCCATCGTGAACAAGA	CGTCTCTGCTTCCCGGTAGTA

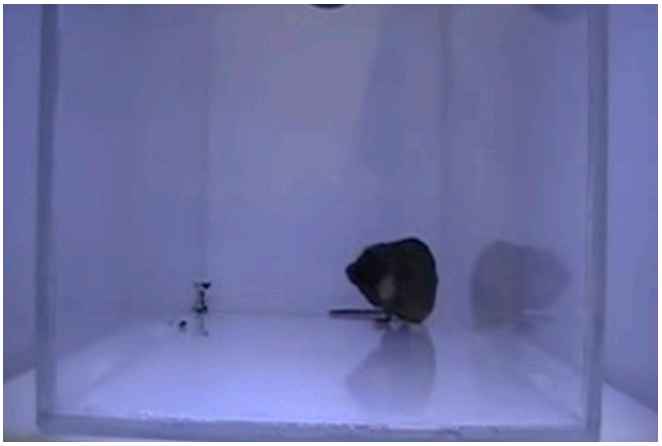

Movie S1. Stereotypic grooming behavior in a mouse after DLS ChAT interneuron ablation under acute startle stress.

Movie S1

Movie S2. Locomotor and stereotypical behavior after amphetamine challenge. The two mice on the *Left* have undergone DLS ChAT interneuron ablation; the one on the *Right* is a control.

Movie S2